

**Thin films of electron donor-acceptor complexes:  
characterisation of mixed-crystalline phases and implications for electrical doping**

Andreas Opitz,<sup>1\*</sup> Giuliano Duva,<sup>2</sup> Marius Gebhardt,<sup>3</sup> Hongwon Kim,<sup>3</sup> Eduard Meister,<sup>3</sup>  
Tino Meisel,<sup>1</sup> Paul Beyer,<sup>1</sup> Valentina Belova,<sup>2</sup> Christian Kasper,<sup>4</sup> Jens Pflaum,<sup>4</sup> Linus Pithan,<sup>5</sup>  
Alexander Hinderhofer,<sup>2</sup> Frank Schreiber,<sup>2\*</sup> Wolfgang Brütting<sup>3\*</sup>

1. Institut für Physik, Humboldt-Universität zu Berlin
2. Institut für Angewandte Physik, Universität Tübingen
3. Institut für Physik, Universität Augsburg
4. Experimentelle Physik VI, Julius-Maximilians-Universität Würzburg
5. European Synchrotron Radiation Facility, Grenoble

\* Corresponding authors: [Andreas.Opitz@hu-berlin.de](mailto:Andreas.Opitz@hu-berlin.de)  
[Frank.Schreiber@uni-tuebingen.de](mailto:Frank.Schreiber@uni-tuebingen.de)  
[Wolfgang.Brueetting@physik.uni-augsburg.de](mailto:Wolfgang.Brueetting@physik.uni-augsburg.de)

---

**Supporting information**

---

**1. Experimental and calculational details**

Single-component and co-deposited films were prepared by vacuum sublimation in high vacuum conditions ( $p < 10^{-6}$  mbar) from separated sources. Sequential deposition was applied by spin coating the dopant F4TCNQ from acetonitrile or chlorobenzene onto a single-component film of DBTTF or DIP prepared by vacuum sublimation, respectively. Deposition rates were controlled by quartz microbalances separately. The deposition rates were about  $1 \text{ nm} \cdot \text{min}^{-1}$  or less. The respective molar ratios of D:A films were set due to variation of the individual deposition rates. The acceptor molecules TCNNQ and F6TCNNQ are less volatile than the respective acceptor molecules TCNQ and F4TCNQ with similar reduction potentials. [1] Therefore, a more reliable deposition by vacuum sublimation is possible. UV-vis-NIR absorbance measurements were performed in transmission geometry using a Perkin Elmer Lambda 950 UV/Vis/NIR spectrophotometer or a Sentech SE 850 Ellipsometer using films deposited on glass or quartz glass slides.

Ex situ AFM measurements were performed at a Bruker Dimension Icon in peak force tapping mode (ScanAsyst) using SCANASYST-AIR cantilevers with a typical resonance frequency of 70 kHz and spring constant of  $0.4 \text{ N} \cdot \text{m}^{-1}$ . Background correction and image analysis were done using the software package Gwyddion. [2]

X-ray scattering measurements were carried out at synchrotron facilities using silicon single-crystalline substrates. The data of single-component acceptor films were taken at The European Synchrotron Radiation Facility (ESRF, beamline ID10) with a beam energy of 14 keV. The ESRF beamline ID03 was used to measure the DBTTF film and the co-deposited D:A films containing DBTTF with a beam energy of 22 keV. The measurements of the single component DIP and the DIP:TCNNQ co-deposited films were performed at the Swiss Light Source (SLS, beamline X04SA) with a beam energy of 14 keV. Grazing incidence x-ray diffraction (GIXD) measurements were performed at an incidence angle of approx. 80-90% of critical angle of silicon at the given energy. The films before and after sequential deposition of F4TCNQ were characterised using a Seifert 3003 PTS diffractometer applying the  $\text{Cu K}\alpha_1$  line.

Raman spectroscopy was performed at different systems based on micro photoluminescence setups. An excitation wavelength of 532 nm was used in all cases. The DBTTF film was measured at 77 K substrate temperature in dry nitrogen atmosphere, all other films were measured at room temperature. Fourier-transformed infra-red spectroscopy was performed in vacuo using a Bruker IFS-66v spectrometer with a mid-range mercury cadmium telluride detector cooled with liquid nitrogen in

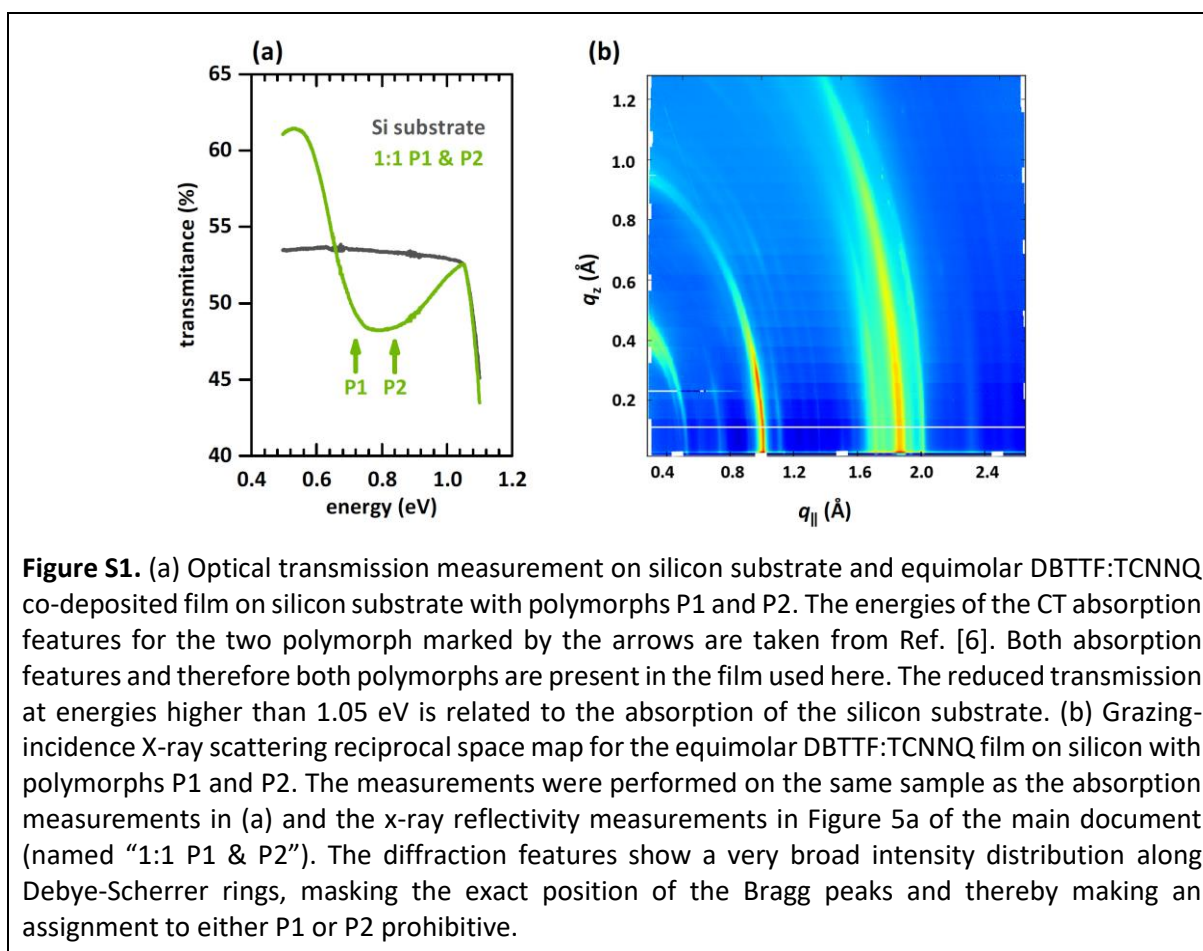
transmission geometry and normal incidence. Additionally, infra-red spectroscopy was performed with grazing incidence ( $80^\circ$  to normal incidence) in transmission (p-polarised light) and reflection (s-polarised light) using Vertex 70 infrared spectrometer. Samples were prepared on non-doped silicon wafers (Siegert prime grade, 1 mm thickness, native oxide, used as received).

Room-temperature conductivity measurements were carried out for films deposited on glass substrates with pre-patterned, interdigitated indium tin oxide contacts (channel length  $50\ \mu\text{m}$ , different channel widths due to application of shadow mask during evaporation of molecular materials) purchased from Ossila Ltd. using a Keithley SourceMeter 2612A in the dark. Several of these in-plane devices (2-5) were measured in two-terminal geometry for each molar ratio.

Temperature-dependent conductivity measurements were performed under high vacuum in a liquid nitrogen cooled cryostat from CryoVac GmbH & Co. KG using a Keithley parameter analyser 4200-SCS. The conductivity of the organic film was analysed by transfer-length method. [3] Silver electrodes were deposited on top of the organic film by vacuum sublimation. The activation energy was determined in the temperature range around room temperature

Density functional theory (DFT) calculations (6-31G\*\* basis set) on isolated molecules employed the long-range corrected  $\omega\text{B97X-D}$  exchange-correlation functional for full geometry optimization, as it contains semi-empirical van der Waals corrections [4], and the PBE0 hybrid functional [5] to subsequently compute vibrational transitions with time-dependent DFT.

## 2. Supporting figures and table



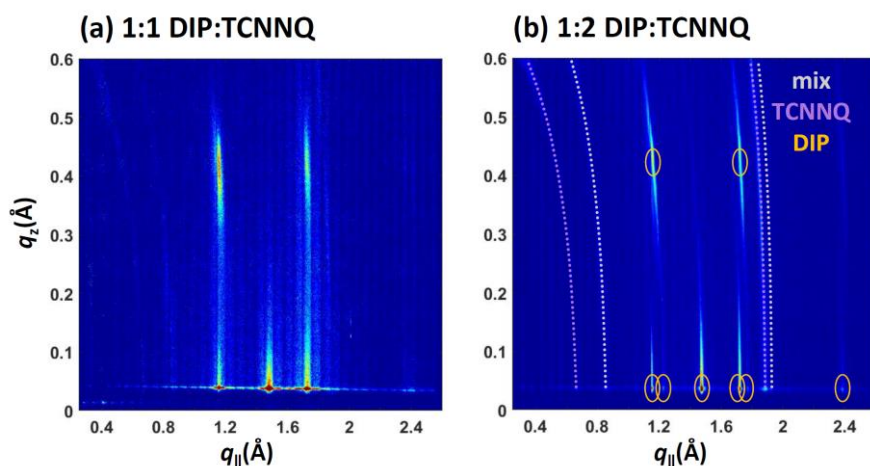


**Figure S2.** X-ray scattering reciprocal space maps for co-deposited films DIP:TCNNQ molar ratios (a) 1:1 and (b) 1:2. The measurements were performed on the samples as shown in Figure 9 of the main document. Labels are given only for measurements on the acceptor rich films. The DIP Bragg peaks are slightly elongated, indicating not perfectly 2D-texture of the DIP domains. The diffraction features related to the mixed crystal ("mix") and to TCNNQ resemble Debye-Scherrer rings, indicating a rather 3D-texture of these domains. The Bragg features related to the mixed crystal ("mix") and to TCNNQ are present as rings, indicating a powder like structure.

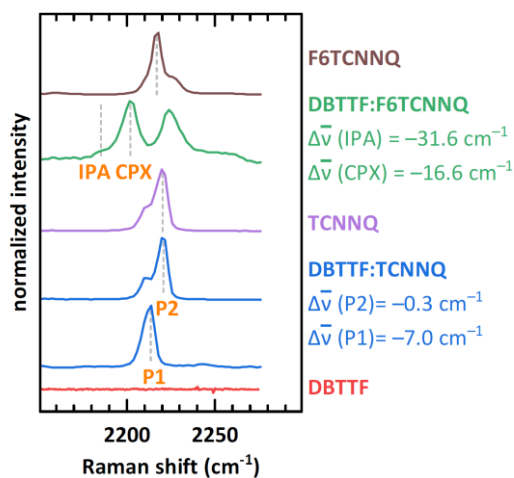


**Figure S3.** Raman spectra for single component and co-deposited D:A films of DBTTF, TCNNQ and F6TCNNQ. The shown region corresponds to the stretching mode of the C≡N vibration. The determined shift of the vibrational energies and the resulting degrees of CT are comparable to infrared transmission measurements. [6] The resulting degrees of CT are summarized in Table S1.

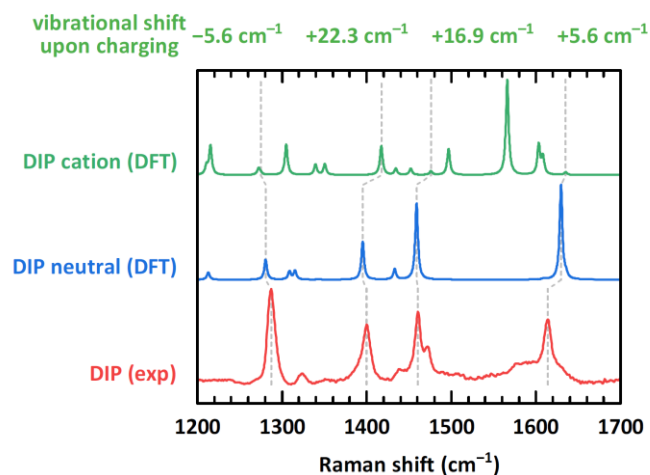


**Figure S4:** Experimental (exp) and calculated (DFT) Raman spectra for neutral DIP together with the calculated Raman spectrum of DIP cation. The energy scale of the calculated spectra is multiplied by 0.95569 to fit the region of experimental data. The associated energies of the most prominent  $A_g$  modes in the different spectra are given by the grey dashed lines. The calculated vibrational shifts of these  $A_g$  modes upon charging the DIP molecule positively are given above the diagram. Differences in the spectra of the neutral DIP are related to the molecular geometry, which is a thin film in experiment and an isolated molecule in DFT calculations. The marked low Raman shift vibration of the neutral molecule is present as high energy shoulder (marked energy by dashed line) close to the peak present in the calculated Raman spectrum of DIP cation.

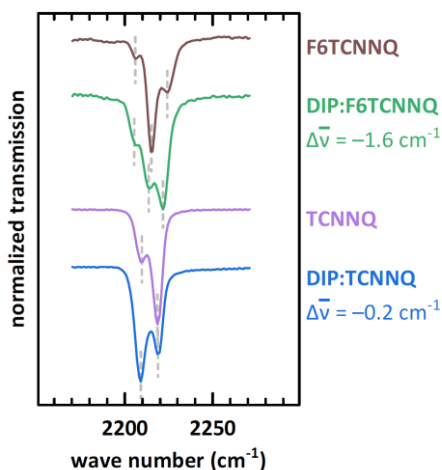


**Figure S5:** Fourier transformed infra-red (FTIR) spectroscopy data for the region of the  $C\equiv N$  stretching vibration of single-component A and co-deposited D:A films for DIP, TCNNQ and F6TCNNQ. The given values for the peak shift are an averaged number considered all indicated positions for one respective acceptor material. The shift for integer charge transfer is about  $-31.3 \text{ cm}^{-1}$  as determined by FTIR measurements on co-deposited films DBTTF:F6TCNNQ. [6] In both cases the number of observed peaks stays constant, the change of relative intensities is related to change of environment from single component to co-deposited films.

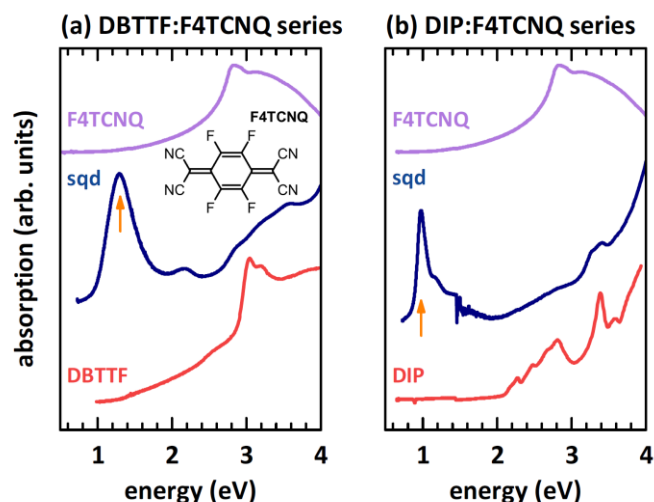


**Figure S6.** Absorption spectra of single component films of DIP, DBTTF and F4TCNQ together with films prepared from DIP and DBTTF films with sequential deposition (sqd) of F4TCNQ. The CT absorption energy are marked by orange arrows. The single component films were prepared by vacuum sublimation. The inset in (a) shows the chemical structure of F4TCNQ. The strong background for the DBTTF single-component film is related to the high roughness and inhomogeneous coverage for the characterised film.

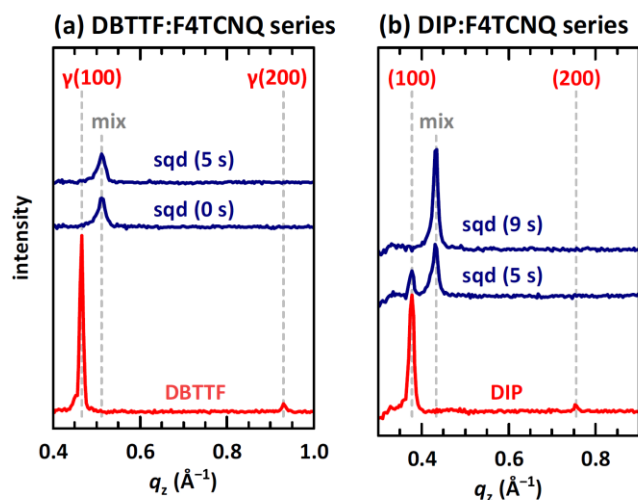


**Figure S7.** X-ray reflectivity measurements for single component of DBTTF (a) and DIP (b) together with x-ray reflectivity measurements for sequentially deposited (sqd) F4TCNQ on such single component films. The numbers given in parentheses is the waiting time after putting the drop of F4TCNQ solution, before starting the spin coater. Acetonitrile and chlorobenzene were used to deposit the F4TCNQ on DBTTF and DIP, respectively. The Bragg peaks of the single component films correspond to the structures described in the main text. The Bragg peaks marked as “mix” are related to the mixed crystals formed here. The absence of the Bragg peaks of donor material after sqd might be related to the change of molecular arrangement and crystallite orientation due to solvent treatment, as observed, e.g. by solvent vapour annealing of DIP before. [7]

**Table S1.** Frequency shift for the C≡N stretching mode of TCNNQ and F6TCNNQ in co-deposited D:A films with DBTTF. The frequency shift determined by Fourier transformed infra-red (IR) spectroscopy are taken from ref. [6]. The data from Raman measurements are shown in Figure S3. The vibrational shifts of integer charge transfer (ICT) from FTIR and Raman measurements are taken as reference to calculate the degree of CT [8] for the EDA CPXs, respectively. A reasonable agreement was found between the degree of CT determined by the two different measurement techniques. As mentioned already in [6], taking the a linear relation between frequency shift and degree of CT [8] by neglecting electron-molecular vibration coupling can lead to overestimation of the degree of CT. [9,10]

material combination	frequency shift (cm <sup>-1</sup> )		degree of charge transfer	
	IR [6]	Raman	IR [6]	Raman
DBTTF:F6TCNNQ ICT	-31.3	-31.6	1	1
DBTTF:F6TCNNQ CPX	-19.4	-16.6	0.62	0.53
DBTTF:TCNNQ P1	-8.8	-7.0	0.28	0.22
DBTTF:TCNNQ P2	0	-0.3	0	0.01

**Table S2:** Conductivity and activation energy for single-component, co-deposited and sequentially deposited films as shown in Figure 12 of the manuscript. The films doped with F6TCNNQ as acceptor were prepared by co-evaporation, sequential deposition was applied for F4TCNQ as acceptor material. All measurements were performed in in-plane geometry.

material combination	electrical conductivity (S/m)	activation energy (eV)
DIP	$(4.7 \pm 0.5) \cdot 10^{-7}$	823 ± 4
DBTTF	$(3.0 \pm 0.3) \cdot 10^{-7}$	819 ± 3
6T	$(1.6 \pm 0.2) \cdot 10^{-5}$	900 ± 30
F6TCNNQ	$(2.9 \pm 0.3) \cdot 10^{-7}$	650 ± 30
DIP:F6TCNNQ 10:1	$(3.6 \pm 0.2) \cdot 10^{-7}$	630 ± 20
DIP:F6TCNNQ 3:2	$(7 \pm 4) \cdot 10^{-6}$	303 ± 4
DIP:F6TCNNQ 1:1	$(4 \pm 2) \cdot 10^{-5}$	400 ± 6
DIP:F4TCNQ	$(1.8 \pm 0.1) \cdot 10^{-3}$	197 ± 6
DBTTF:TCNNQ 10:1 [6]	$3 \cdot 10^{-2}$	171
DBTTF:F6TCNNQ 10:1	$(2.7 \pm 0.4) \cdot 10^{-2}$	131 ± 1
DBTTF:F6TCNNQ 10:1 [6]	$2.4 \cdot 10^0$	100
DBTTF:F6TCNNQ 3:2	$(3.1 \pm 0.3) \cdot 10^0$	124 ± 1
DBTTF:F6TCNNQ 1:1	$(4 \pm 2) \cdot 10^{-4}$	151 ± 2
DBTTF:F4TCNQ	$(4 \pm 3) \cdot 10^{-2}$	200 ± 5
6T:F6TCNNQ 10:1	$(3 \pm 1) \cdot 10^{-2}$	307 ± 2
6T:F6TCNNQ 3:1	$(2.1 \pm 0.1) \cdot 10^{-1}$	110 ± 3
6T:F6TCNNQ 1:1	$(1.3 \pm 0.1) \cdot 10^{-1}$	212 ± 7

### 3. References

- [1] B. Wegner, L. Grubert, C. Dennis, A. Opitz, A. Röttger, Y. Zhang, S. Barlow, S.R. Marder, S. Hecht, K. Müllen, N. Koch, Predicting the yield of ion pair formation in molecular electrical doping: redox-potentials versus ionization energy/electron affinity, *J. Mater. Chem. C* 7 (2019) 13839–13848. doi:10.1039/C9TC04500G.
- [2] D. Nečas, P. Klapetek, Gwyddion: an open-source software for SPM data analysis, *Open Phys.* 10 (2012) 181–188. doi:10.2478/s11534-011-0096-2.
- [3] S. Luan, G.W. Neudeck, An experimental study of the source/drain parasitic resistance effects in amorphous silicon thin film transistors, *J. Appl. Phys.* 72 (1992) 766–772. doi:10.1063/1.351809.
- [4] J.-D. Chai, M. Head-Gordon, Long-range corrected hybrid density functionals with damped atom–atom dispersion corrections, *Phys. Chem. Chem. Phys.* 10 (2008) 6615. doi:10.1039/b810189b.
- [5] C. Adamo, V. Barone, Toward reliable density functional methods without adjustable parameters: The PBE0 model, *J. Chem. Phys.* 110 (1999) 6158–6170. doi:10.1063/1.478522.
- [6] P. Beyer, D. Pham, C. Peter, N. Koch, E. Meister, W. Brütting, L. Grubert, S. Hecht, D. Nabok, C. Cocchi, C. Draxl, A. Opitz, State-of-Matter-Dependent Charge-Transfer Interactions between Planar Molecules for Doping Applications, *Chem. Mater.* 31 (2019) 1237–1249. doi:10.1021/acs.chemmater.8b01447.
- [7] S. Grob, A.N. Bartynski, A. Opitz, M. Gruber, F. Grassl, E. Meister, T. Linderl, U. Hörmann, C. Lorch, E. Moons, F. Schreiber, M.E. Thompson, W. Brütting, Solvent vapor annealing on perylene-based organic solar cells, *J. Mater. Chem. A* 3 (2015) 15700–15709. doi:10.1039/C5TA02806J.
- [8] J.S. Chappell, A.N. Bloch, W.A. Bryden, M. Maxfield, T.O. Poehler, D.O. Cowan, Degree of charge transfer in organic conductors by infrared absorption spectroscopy, *J. Am. Chem. Soc.* 103 (1981) 2442–2443. doi:10.1021/ja00399a066.
- [9] A. Girlando, Comment on Polymorphism in the 1:1 Charge-Transfer Complex DBTT-TCNQ and Its Effects on Optical and Electronic Properties, *Adv. Electron. Mater.* 3 (2017) 1600437. doi:10.1002/aelm.201600437.
- [10] A. Girlando, A. Painelli, C. Pecile, Electron-Intramolecular Phonon Coupling in regular and Dimerized Mixed Stack Organic Semiconductors, *Mol. Cryst. Liq. Cryst.* 120 (2007) 17–26. doi:10.1080/00268948508075754.